

# The equation of state in two-, three-, and four-color QCD at non-zero temperature and density

Tyler Gorda and Paul Romatschke<sup>1</sup>

<sup>1</sup>*University of Colorado Boulder, Boulder, CO*

(Dated: October 10, 2018)

We calculate the equation of state at non-zero temperature and density from first principles in two-, three- and four-color QCD with two fermion flavors in the fundamental and two-index, antisymmetric representation. By matching low-energy results (from a ‘hadron resonance gas’) to high-energy results from (resummed) perturbative QCD, we obtain results for the pressure and trace anomaly that are in quantitative agreement with full lattice-QCD studies for three colors at zero chemical potential. Our results for non-zero chemical potential at zero temperature constitute predictions for the equation of state in QCD-like theories that can be tested by traditional lattice studies for two-color QCD with two fundamental fermions and four-color QCD with two two-index, antisymmetric fermions. We find that the speed of sound squared at zero temperature can exceed one third, which may be relevant for the phenomenology of high-mass neutron stars.

## I. INTRODUCTION

Knowledge about condensed-matter properties of quantum chromodynamics (QCD) in thermodynamic equilibrium is required for the interpretation of experimental and observational data in cosmology, high-energy nuclear physics and the physics of neutron stars. While tremendous progress has been made for the case of high temperature and small baryon densities using direct simulations in lattice QCD [1–3], much less is known for the case of small temperature and large densities. The reason for this shortcoming is that the so-called sign problem prohibits the direct simulation of QCD (which is an SU(3) gauge theory with  $n_f = 2 + 1$  fundamental fermionic degrees of freedom) at large density using established importance sampling techniques. While established techniques fail, several recent techniques have been studied that at least in principle could permit one to calculate thermodynamic properties from first principles in QCD at large density. These techniques include Lefschetz thimbles [4], complex Langevin [5–8], strong coupling expansion [9], and hadron resonance gas plus perturbative QCD (“HRG+pQCD” in the following) [10–12]. In this work, we propose a series of ‘control studies’ in QCD-like theories (in particular two-color QCD with two fundamental flavors and four-color QCD with two flavors in the two-index, antisymmetric representation), which—despite not corresponding to the actual theory of strong interactions realized in nature—have the advantage of not suffering from a sign problem, and are thus amenable to direct simulations using established lattice-QCD techniques. We then proceed to calculate thermodynamic properties in these QCD-like theories in one of the above non-traditional approaches (HRG+pQCD, Ref. [10–12]), which effectively makes predictions for possible future lattice-QCD studies that can be used to validate or falsify this HRG+pQCD approach. Since two- and four-color QCD are qualitatively similar to three-color QCD, we furthermore expect the level of agreement between lattice QCD and HRG+pQCD in the two- or four-color cases to be roughly comparable to the three-color QCD case, thus offering an indirect validation of non-traditional methods for QCD at large densities.

The paper is organized as follows. In Section II we review the HRG+pQCD method and give the equation of state in pQCD by stating the pressure  $P$  as a function of temperature  $T$  at baryon chemical potential  $\mu = 0$  and  $P$  as a function of  $\mu$  at  $T = 0$ . This section is essentially a compilation of what has been derived in the literature. In Section III we compute the HRG pressure as a function of  $T$  or  $\mu$ . The former case is simple and is derived quickly, whereas the latter is derived in more detail, especially for the theories where the baryons of the theory are bosons. This section also contains an explanation of how the hadrons in the theories listed above are computed. Section IV contains a description of how we perform the matching between these two asymptotic equations of state, and in Section V we discuss our results.

## II. PQCD EQUATION OF STATE

In this work, we are interested in calculating the pressure  $P$  along the  $\mu = 0$  and  $T = 0$  axes in the theories  $(N, n_f) = (2, 2), (3, 3),$  and  $(4, 2)$  with quarks in the fundamental representation (fundamental) and  $(4, 2)$  with quarks in the two-index, antisymmetric representation (antisymmetric). In order to constrain the pressure of these theories, we derive the asymptotic behavior for both low and high  $T$  or  $\mu$  and then match these behaviors using basic thermodynamics. At high  $T$  or high  $\mu$ , the equation of state can be calculated using (resummed) pQCD and at low  $T$  or  $\mu$ , the equation of state of the theory is to good approximation [1–3, 13] that of a HRG (a noninteracting collection of the hadrons of

that theory). In the intermediate regime, the equations of state can be constructed by matching the high/low energy asymptotic behavior using the criterion that the pressure  $P$  must increase as a function of  $T$  or as a function of  $\mu$  (see [14]). More details of the matching procedure will be discussed below. Throughout this paper, Boltzmann's constant  $k$ , Planck's reduced constant  $\hbar$ , and the speed of light  $c$  will be set equal to one.

The high- $T$ , pQCD equation of state can be calculated by following the equations and procedure of Kajantie *et al.* [15, 16] and Vuorinen [14] with the resummation modifications described by Blaizot *et al.* [17] (cf. Ref. [18] for a different approach to the resummed pQCD equation of state). We first define the following group-theory terms to be used in all future pQCD expressions:

$$C_A = N, \quad (II.1)$$

$$d_A = N^2 - 1, \quad (II.2)$$

and

$$C_{\text{fundamental}} = \frac{N^2 - 1}{2N}, \quad C_{\text{antisymmetric}} = \frac{(N - 2)(N + 1)}{N}, \quad (II.3)$$

$$T_{\text{fundamental}} = \frac{n_f}{2}, \quad T_{\text{antisymmetric}} = \frac{(N - 2)}{2} n_f, \quad (II.4)$$

$$d_{\text{fundamental}} = N n_f, \quad d_{\text{antisymmetric}} = \frac{N(N - 1)}{2} n_f. \quad (II.5)$$

In all of the expressions that follow, we let group-theory terms with a subscript  $R$  denote the fermionic group-theory invariants, which must be replaced by the corresponding fundamental or antisymmetric representation group-theory invariants above as needed. In terms of these group-theory terms, the pQCD pressure at  $\mu = 0$  in these theories can be written

$$P_{\text{pQCD}}(T) = P_{\text{sb}}(T) + P_{\text{hard}}(T) + P_{\text{EQCD}}(T). \quad (II.6)$$

Here, the  $P_{\text{sb}}$  the Stefan-Boltzmann pressure given by

$$P_{\text{sb}}(T) = \frac{\pi^2 T^4}{45} \left( d_A + \frac{7}{4} d_R \right). \quad (II.7)$$

To 3-loop order,  $P_{\text{hard}}$  is given by Braaten and Nieto [19] as

$$\begin{aligned} P_{\text{hard}}(T) = & \frac{\pi^2 d_A T^4}{9} \left\{ - \left( C_A + \frac{5}{2} T_R \right) \frac{\alpha_s}{4\pi} \right. \\ & + \left( C_A^2 \left[ 48 \ln \frac{\Lambda_E}{4\pi T} - \frac{22}{3} \ln \frac{\bar{\Lambda}}{4\pi T} + \frac{116}{5} + 4\gamma + \frac{148}{3} \frac{\zeta'(-1)}{\zeta(-1)} - \frac{38}{3} \frac{\zeta'(-3)}{\zeta(-3)} \right] \right. \\ & + C_A T_R \left[ 48 \ln \frac{\Lambda_E}{4\pi T} - \frac{47}{3} \ln \frac{\bar{\Lambda}}{4\pi T} + \frac{401}{60} - \frac{37}{5} \ln 2 + 8\gamma + \frac{74}{3} \frac{\zeta'(-1)}{\zeta(-1)} - \frac{1}{3} \frac{\zeta'(-3)}{\zeta(-3)} \right] \\ & + T_R^2 \left[ \frac{20}{3} \ln \frac{\bar{\Lambda}}{4\pi T} + \frac{1}{3} - \frac{88}{5} \ln 2 + 4\gamma + \frac{16}{3} \frac{\zeta'(-1)}{\zeta(-1)} - \frac{8}{3} \frac{\zeta'(-3)}{\zeta(-3)} \right] \\ & \left. \left. + C_R T_R \left[ \frac{105}{4} - 24 \ln 2 \right] \right) \left( \frac{\alpha_s}{4\pi} \right)^2 \right\}, \quad (II.8) \end{aligned}$$

where  $\Lambda_E$  is the factorization scale between the hard and soft modes, and  $\alpha_s$  is the strong coupling constant squared over  $4\pi$  in the  $\overline{\text{MS}}$  renormalization scheme at the scale  $\bar{\Lambda} = \sqrt{(2\pi T)^2 + (\mu)^2}$ . This is given by [12, 20]

$$\alpha_s(\bar{\Lambda}) = \frac{4\pi}{\beta_0 L} \left( 1 - \frac{\beta_1}{\beta_0^2} \frac{\ln L}{L} \right), \quad L = \ln \left( \bar{\Lambda}^2 / \Lambda_{\overline{\text{MS}}}^2 \right), \quad (II.9)$$

with

$$\beta_0 = \frac{11}{3} C_A - \frac{4}{3} T_R, \quad \beta_1 = \frac{34}{3} C_A^2 - 4 C_R T_R - \frac{20}{3} C_A T_R, \quad (II.10)$$

where  $\Lambda_{\overline{\text{MS}}}$  is the  $\overline{\text{MS}}$  renormalization point (to be set later). In all our results, we set  $\Lambda_E = \bar{\Lambda}$  and vary  $\bar{\Lambda}$  about the aforementioned value by a factor of two (cf. the end of Section IV). Finally,  $P_{\text{EQCD}}$  is given by

$$P_{\text{EQCD}}(T) = \frac{d_A}{4\pi} T \left( \frac{1}{3} m_E^3 - \frac{C_A}{4\pi} \left( \ln \frac{\Lambda_E}{2m_E} + \frac{3}{4} \right) g_E^2 m_E^2 - \left( \frac{C_A}{4\pi} \right)^2 \left( \frac{89}{24} - \frac{11}{6} \ln 2 + \frac{1}{6} \pi^2 \right) g_E^4 m_E \right), \quad (II.11)$$

where

$$\begin{aligned}
m_E^2 = & \frac{4\pi}{3} \alpha_s T^2 \left\{ C_A + T_R \right. \\
& + \left[ C_A^2 \left( \frac{5}{3} + \frac{22}{3} \gamma + \frac{22}{3} \ln \frac{\bar{\Lambda}}{4\pi T} \right) + C_A T_R \left( 3 - \frac{16}{3} \ln 2 + \frac{14}{3} \gamma + \frac{14}{3} \ln \frac{\bar{\Lambda}}{4\pi T} \right) \right. \\
& \left. \left. + T_R^2 \left( \frac{4}{3} - \frac{16}{3} \ln 2 - \frac{8}{3} \gamma - \frac{8}{3} \ln \frac{\bar{\Lambda}}{4\pi T} \right) - 6C_R T_R \right] \left( \frac{\alpha_s}{4\pi} \right) \right\}, \tag{II.12}
\end{aligned}$$

and

$$g_E^2 = 4\pi \alpha_s T. \tag{II.13}$$

The  $T = 0$ , pQCD equation of state is more straightforward in the sense that resummation of the strict perturbative series is not required. The result is given in Ref. [14] by

$$\begin{aligned}
P_{\text{pQCD}}(\mu) = & \frac{1}{4\pi^2} \left( \sum_f \mu_f^4 \left\{ \frac{d_R}{3n_f} - d_A \left( \frac{2T_R}{n_f} \right) \left( \frac{\alpha_s}{4\pi} \right) - d_A \left( \frac{2T_R}{n_f} \right) \left( \frac{\alpha_s}{4\pi} \right)^2 \left[ \frac{2}{3} (11C_A - 4T_R) \ln \frac{\bar{\Lambda}}{\mu_f} + \frac{16}{3} \ln 2 \right. \right. \right. \\
& \left. \left. + \frac{17}{4} \left( \frac{C_A}{2} - C_R \right) + \frac{1}{36} (415 - 264 \ln 2) C_A - \frac{8}{3} \left( \frac{11}{6} - \ln 2 \right) T_R \right] \right\} \right. \\
& \left. - d_A \left( \frac{2T_R}{n_f} \right) \left( \frac{\alpha_s}{4\pi} \right)^2 \left\{ \left( 2 \ln \frac{\alpha_s}{4\pi} - \frac{22}{3} + \frac{16}{3} \ln 2 (1 - \ln 2) + \delta + \frac{2\pi^2}{3} \right) (\mu^2)^2 + F(\mu) \right\} \right) \\
& + \mathcal{O}(\alpha_s^3 \ln \alpha_s), \tag{II.14}
\end{aligned}$$

where the sum is over all the quark flavors in the theory,  $\mu_f$  is the  $f$ -quark chemical potential,  $\mu^2 = \sum_f \mu_f^2$ , and

$$\begin{aligned}
F(\mu) = & -2\mu^2 \left( \frac{2T_R}{n_f} \right) \sum_f \mu_f^2 \ln \frac{\mu_f^2}{\mu^2} + \frac{2}{3} \left( \frac{2T_R}{n_f} \right)^2 \sum_{f>g} \left\{ (\mu_f - \mu_g)^2 \ln \frac{|\mu_f^2 - \mu_g^2|}{\mu_f \mu_g} \right. \\
& \left. + 4\mu_f \mu_g (\mu_f^2 + \mu_g^2) \ln \frac{(\mu_f + \mu_g)^2}{\mu_f \mu_g} - (\mu_f^4 - \mu_g^4) \ln \frac{\mu_f}{\mu_g} \right\}, \tag{II.15}
\end{aligned}$$

with the constant  $\delta$  having the value  $\delta = 0.85638320933$ . In what follows we always set all of the quark chemical potentials equal to each other, so that  $\mu_f = \mu/N_b$  for each flavor  $f$ , where  $N_b$  is the number of quarks in a baryon. Note that this means that some of the terms in (II.15) do not contribute.

### III. HADRON RESONANCE GAS EQUATION OF STATE

The low- $T$  pressure in these theories is given by considering the system to be a free gas of hadrons. Moreover, the statistics of the hadrons may be ignored, so that the distribution functions may all be assumed to be Boltzmann factors. In that case, we have

$$P_{\text{HRG}}(T) = T \sum_{i \in H} g_i \int \frac{d^3 p}{(2\pi)^3} e^{-\sqrt{\mathbf{p}^2 + m_i^2}/T} = T^4 \sum_{i \in H} \frac{g_i}{2\pi^2} \left( \frac{m_i}{T} \right)^2 K_2 \left( \frac{m_i}{T} \right), \tag{III.1}$$

where here the sum is over the hadron spectrum of the theory;  $g_i$  and  $m_i$  are the degeneracy and the mass of the  $i$ th particle, respectively;  $\mathbf{p} = |\vec{p}|$ ; and  $K_2$  is a modified Bessel function of the second kind.

The low- $\mu$  pressure can be calculated in a similar way, but in this case the statistics of the particles cannot be ignored. For  $T = 0$  and  $\mu > 0$ , the only particles that contribute to the partition function are particles containing no antiquarks, which we denote by  $B$ . In all the fundamental theories, these are simply the baryons, whereas for the antisymmetric theory there are more particles fitting this description (see below). As such, in this section we shall refer to all the particles in  $B$  as baryons. Taking the  $T \rightarrow 0$  limit in the fermionic-baryon ( $\eta = 1$ ) or bosonic-baryon

( $\eta = -1$ ) case yields

$$\begin{aligned}
P_{\text{HRG}}(\mu) &= \lim_{T \rightarrow 0} T \sum_{i \in B} g_i \eta \int \frac{d^3 p}{(2\pi)^3} \ln \left( 1 + \eta e^{(\mu r_i - \sqrt{\mathbf{p}^2 + m_i^2})/T} \right) \\
&= \sum_{i \in B} g_i \eta \int \frac{d^3 p}{(2\pi)^3} \ln \left[ \lim_{T \rightarrow 0} \left( 1 + \eta e^{(\mu r_i - \sqrt{\mathbf{p}^2 + m_i^2})/T} \right)^T \right] \\
&= \sum_{i \in B} g_i \eta \int_0^{\sqrt{(\mu r_i)^2 - m_i^2}} \frac{\mathbf{p}^2 d\mathbf{p}}{2\pi^2} \left( \mu r_i - \sqrt{\mathbf{p}^2 + m_i^2} \right) \theta(\mu r_i - m_i) \\
&= \eta \sum_{i \in B} \frac{g_i}{48\pi^2} \left[ \mu r_i \sqrt{(\mu r_i)^2 - m_i^2} (2(\mu r_i)^2 - 5m_i^2) + 3m_i^4 \cosh^{-1} \left( \frac{m_i}{\sqrt{(\mu r_i)^2 - m_i^2}} \right) \right] \theta(\mu r_i - m_i), \quad (\text{III.2})
\end{aligned}$$

where here  $\theta$  is the Heaviside step function and  $r_i = N_i/N_b$ , with  $N_i$  being the number of quarks in the  $i$ th particle. This result is correct for the fermionic-baryon case, but this formula gives negative  $P$  in the bosonic-baryon case when  $\mu > \min_{i \in B} m_i/r_i$ . This is because, in the bosonic case, a condensate of the  $i$ th baryon forms when  $\mu = m_i/r_i$ . (This has been numerically investigated in the two-color case by Hands *et al.* [21] and analytically by Kogut *et al.* [22] in all QCD-like theories with pseudoreal fermions.) In fact, in the completely-noninteracting case it is nonsensical for  $\mu$  to exceed  $\min_{i \in B} m_i/r_i$ . Since the hadrons in these theories are composite particles, they are not truly noninteracting, and we can have  $\mu > \min_{i \in B} m_i/r_i$ .

To make sense of this case, we consider the bosons as a (complex) quantum field  $\Phi$  with a  $|\Phi|^4$  repulsive interaction. For simplicity, we consider each baryon to be an independent field, and we examine the case of a scalar field (degeneracies may easily be incorporated at the end). A single baryon then has the Lagrangian density (in the mostly minus convention)

$$\mathcal{L} = (\partial_\mu \Phi^\dagger)(\partial^\mu \Phi) - m^2 \Phi^\dagger \Phi - \lambda (\Phi^\dagger \Phi)(\Phi^\dagger \Phi), \quad (\text{III.3})$$

with  $\lambda > 0$ . Following Kapusta and Gale [23], we introduce a baryon chemical potential  $\mu r$  and explicitly factor out the zero momentum mode

$$\Phi = \xi + \chi, \quad (\text{III.4})$$

where  $\xi \in \mathbb{R}$  is a constant and the constant Fourier component of  $\chi$  satisfies  $\chi_{n=0}(\mathbf{p} = 0) = 0$ . One may think of  $\xi$  as the condensate field and  $\chi$  as the fluctuations about the vacuum state. We also write the fluctuations in terms of the normalized real and imaginary parts

$$\chi = \frac{1}{\sqrt{2}}(\chi_1 + i\chi_2). \quad (\text{III.5})$$

In terms of these new variables, the Euclidean Lagrangian density becomes

$$\begin{aligned}
\mathcal{L} &= -\frac{1}{2} \left( \frac{\partial \chi_1}{\partial \tau} - i\mu r \chi_2 \right)^2 - \frac{1}{2} \left( \frac{\partial \chi_2}{\partial \tau} + i\mu r \chi_1 \right)^2 - \frac{1}{2} \nabla^2 \chi_1 - \frac{1}{2} \nabla^2 \chi_2 \\
&\quad - \frac{1}{2} (6\lambda \xi^2 + m^2) \chi_1^2 - \frac{1}{2} (2\lambda \xi^2 + m^2) \chi_2^2 - U(\xi) + \mathcal{L}_1, \quad (\text{III.6})
\end{aligned}$$

where  $\tau$  is the Euclidean time,  $\mathcal{L}_1$  contains interacting terms in  $\chi$  (which we henceforth ignore), and

$$U(\xi) = (m^2 - (\mu r)^2) \xi^2 + \lambda \xi^4. \quad (\text{III.7})$$

We thus see from (III.7) that for  $\mu r < m$  the state  $\xi_0 = 0$  is the stable vacuum and (III.6) describes a system of particles and antiparticles of equal masses. However, for  $\mu r > m$ , the stable vacuum becomes

$$\xi_0^2 = \frac{(\mu r)^2 - m^2}{2\lambda}, \quad (\text{III.8})$$

and (III.6) describes a collection of two particles with differing masses:  $\bar{m}_1^2 = 3(\mu r)^2 - 2m^2$  and  $\bar{m}_2^2 = (\mu r)^2$  respectively. Because of the chemical potential, the dispersion relation of the latter is gapless, and Goldstone's theorem is satisfied. At zero temperature, the pressure is simply

$$P_{\text{HRG}}(\mu) = U(\xi) \Big|_{\xi=\xi_0} = \frac{1}{4\lambda} ((\mu r)^2 - m^2)^2 \theta(\mu r - m). \quad (\text{III.9})$$

This gives us the dependence of the pressure on  $\mu$ , but we still have not set the coupling constant  $\lambda$ . We set it as follows. According to (II.14), we see that the Fermi–Dirac pressure for a quark in the theory  $(N, n_f)$  with representation  $R$  becomes

$$P_{\text{fd}} = \frac{d_R}{12\pi^2} \left( \frac{\mu r}{N_b} \right)^4, \quad (\text{III.10})$$

so that for a single degree of freedom (recalling that a fermionic quark has two degrees of freedom) one has

$$P_{\text{fd}} = \frac{1}{24\pi^2 N_b^4} (\mu r)^4. \quad (\text{III.11})$$

Thus, in order for  $P_{\text{HRG}} \rightarrow P_{\text{fd}}$  when  $\mu \rightarrow \infty$ , we must have for a single scalar baryon

$$P_{\text{HRG}}(\mu) = \frac{1}{24\pi^2 N_b^4} ((\mu r)^2 - m^2)^2 \theta(\mu r - m), \quad (\text{III.12})$$

and so for a theory with bosonic baryons we have

$$P_{\text{HRG}}(\mu) = \sum_{i \in B} \frac{g_i}{24\pi^2 N_b^4} ((\mu r_i)^2 - m_i^2)^2 \theta(\mu r_i - m_i). \quad (\text{III.13})$$

### A. Determining the hadron spectrum

For the three-color  $(N, n_f) = (3, 3)$  fundamental case, we use the real world spectrum of hadrons up to 2.25 GeV [24]. For the two- and four-color theories with two fundamental quarks and the four-color theory with two antisymmetric quarks, we determine the hadrons using group-theoretic arguments and Fermi statistics (in the case of objects composed of quarks only). We explicitly ignore the glueballs in these theories because they tend to be more massive than the lightest hadrons [25]. For the two- and four-color theories, we set the scale using the string tension  $\sqrt{\sigma}$  and the relation between the string tension and the  $\overline{\text{MS}}$  renormalization scale  $\Lambda_{\overline{\text{MS}}}$  given in Ref. [26]. However, the ratios  $\Lambda_{\overline{\text{MS}}}/\sqrt{\sigma}$  given in the aforementioned reference are for the pure-gauge theories. To remedy this, we scale these ratios by  $\Lambda_{\overline{\text{MS}}}^{N=3}(n_f=2)/\Lambda_{\overline{\text{MS}}}^{N=3}(n_f=0)$ , determined from Ref. [27]. These lead to the values

$$\Lambda_{\overline{\text{MS}}}^{N=2}(n_f=2)/\sqrt{\sigma} = 1.032 \quad \text{and} \quad \Lambda_{\overline{\text{MS}}}^{N=4}(n_f=2)/\sqrt{\sigma} = 0.723 \quad (\text{III.14})$$

for the fundamental theories. For the three-color theory, we use  $\Lambda_{\overline{\text{MS}}} = 0.378$  GeV, as in [12].

For the four-color antisymmetric theory, we were unable to locate a result for  $\Lambda_{\overline{\text{MS}}}^{N=4}(n_f=2)/\sqrt{\sigma}$  from the lattice in the literature. Since some of the group-theory terms for the antisymmetric theory scale more strongly with the number of colors than the corresponding terms in the fundamental theory, it seems reasonable to expect that  $\Lambda_{\overline{\text{MS}}}$  will scale differently with the number of quark flavors in the antisymmetric theory than in the fundamental theory. Moreover, it would be most accurate to view  $\Lambda_{\overline{\text{MS}}}/\sqrt{\sigma}$  as a free parameter in our HRG+pQCD scheme that must be determined independently from the lattice. In light of these considerations, we have decided to use both the pure-gluon value [26]

$$\Lambda_{\overline{\text{MS}}}^{N=4}/\sqrt{\sigma} = 0.527, \quad (\text{III.15})$$

and the previously-given value of  $\Lambda_{\overline{\text{MS}}}^{N=4}(n_f=2)/\sqrt{\sigma}$  that we use for the four-color fundamental theory for the four-color antisymmetric theory, with the expectation that the true value will lie somewhere near this range.

For both the two- and four-color cases, the mesons are taken to be the analogues of the flavorless mesons that exist in the real world (up to a mass of about 2 GeV) whose masses are written in multiples of the string tension  $\sigma_{\text{SU}(3)} = (420 \text{ MeV})^2$ . In the two-color case, we mainly use the analogues of the real-world mesons, substituting the two-color masses calculated by Bali *et al.* [28] when available. (We also note here that the  $\mu$ -dependence of the two-color spectrum has been studied numerically in Ref. [29] and analytically in Ref. [22], though we do not need this  $\mu$ -dependence for our HRG+pQCD scheme.)

We now discuss in some detail how the non-meson objects in these three cases are determined. For convenience and as a summary of these sections, we list tables for all of the particles that we have included in the SU(2) and SU(4) cases in Appendix A.

### 1. Two-color case

In two-color QCD, the baryons are composed of two quarks with the added simplicity that the masses are degenerate with the corresponding mesons made from the same quarks [30]. Thus, the mass spectrum of the baryons is the same as the mass spectrum of mesons. However, there are fewer mesons than baryons, for there is an additional constraint imposed by Fermi statistics in the case of the baryons. Since we may view the two massless quarks as part of an isospin doublet, one sees that exchanging the two internal quarks in a baryon causes the wavefunction to become multiplied by

$$(-1)^{1+L+S+I}. \quad (\text{III.16})$$

In this equation,  $L$  is the angular momentum quantum number,  $S$  is the spin, and  $I$  is the isospin, with the additional 1 due to the fact that the quarks are in an antisymmetric color singlet. We thus see that for even  $L$  the spin and isospin must be equal ( $S = 0$  implies  $I = 0$  and  $S = 1$  implies  $I = 1$ ), and for odd  $L$  they must be the opposite in order to have a totally antisymmetric wavefunction. (Even though the composite baryon is itself a boson in two-color QCD, it is still a multiparticle state of fundamental fermions.) This information is enough to determine the set of hadrons in (III.1).

### 2. Four-color fundamental case

Baryons in four-color QCD with fundamental fermions consist of four quarks. In this case, to determine the masses  $M$  we use the large- $N$  expansion

$$M(J) = NA + \frac{J(J+1)}{N}B, \quad (\text{III.17})$$

where  $J$  is the total angular momentum of the baryon, and  $A, B$  are constants independent of  $N$  [31, 32]. As pointed out by DeGrand [33] and demonstrated by Appelquist *et al.* [34], a term independent of  $N$  could be used for better agreement. However, we have no way to set the value of that term and thus do not include it.

We find the possible values of  $J$  beginning with the ground-state baryons of zero orbital angular momentum. Since we still have a isospin doublet of massless, spin-one-half quarks, we only need the group-theory expression

$$2 \otimes 2 \otimes 2 \otimes 2 = 5_S \oplus 3_M \oplus 3_M \oplus 3_M \oplus 1_A \oplus 1_A, \quad (\text{III.18})$$

where the  $5_S$  state is fully symmetric, the  $3_M$  states are symmetric in three of the four quarks and antisymmetric in the other, and the  $1_A$  states are pairwise antisymmetric. Since, again, the quarks are in an antisymmetric color singlet, it must be the case that they are in a *symmetric* combination of spin and flavor. This means that there is a spin-2 quintet, a spin-1 triplet, and a spin-0 singlet of ground-state baryons.

We may also determine the first excited states in this simple manner by realizing that for this four-body problem there are three relevant orbital-angular-momentum quantum numbers and the first excited state corresponds to when exactly one of them is one. In order to still be in a completely antisymmetric state, either the spin or the flavor state must now be in one of the  $3_M$  states while the other must be in a  $5_S$  state. This means that there are a quintet of particles with  $S = 1$  and a triplet of particles with  $S = 2$ . Combining these with an orbital angular momentum  $L = 1$  yields three baryonic quintets with  $J = 0, 1, 2$  and three baryonic triplets with  $J = 1, 2, 3$ . We did not determine the baryons for any higher excited states.

### 3. Four-color antisymmetric case

The hadron spectrum in the four-color theory with two antisymmetric quarks consists of two-quark objects: mesons and diquarks; four-quark objects: tetraquarks, di-mesons, and diquark-mesons; and six-quark baryons [35–37]. Since the antisymmetric representation is real, the arguments of Ref. [30] carry through here and one may conclude that all two-quark objects with the same quark content have degenerate masses and that the same holds for the four-quark objects. In addition, the four-quark objects have a mass equal to the sum of their constituent two-quark-object masses [35]. Because of this mass degeneracy, we need not determine how all of the four-quark-object degrees of freedom break up into spin and isospin multiplets; rather, we may simply combine the two-quark-object degrees of freedom in every possible way. One major difference from the two-color case, however, is that in the four-color theory with antisymmetric quarks the color-singlet state for diquarks is *symmetric*. This means that the spin-isospin locking in

this theory is the opposite of the locking in the two-color theory. That is, for odd  $L$  the spin and isospin must be equal ( $S = 0$  implies  $I = 0$  and  $S = 1$  implies  $I = 1$ ), and for even  $L$  they must be opposite. As for the six-quark baryons, we again use the large- $N$  expression (III.17), but with  $N$  replaced by  $N_b = 6$ , the number of quarks in the baryon. We include only the ground-state baryons, where isospin and spin are locked as  $I = J = 3, 2, 1$ , and  $0$  [35].

### B. Chiral symmetry breaking and the Nambu–Goldstone bosons

The lowest-mass particles in all of the aforementioned theories are precisely zero at zero quark mass. This can be understood in terms of the pattern of chiral symmetry breaking in these theories [38]. Consider an  $SU(N)$  gauge theory with  $n_f$  massless fermions. For fermions in a complex representation (such as in the cases  $N \geq 3$  with fundamental fermions), the Lagrangian density possesses the symmetry  $U(n_f) \otimes U(n_f)$ , corresponding to the separate left- and right-handed chiral symmetries, and for real representations (such as any  $N$  with adjoint fermions or  $N = 4$  with antisymmetric fermions) or pseudoreal representations (such as in  $N = 2$  with fundamental fermions), the Lagrangian density possesses the larger symmetry  $U(2n_f)$ . In all of these cases, the axial  $U(1)$  symmetry is broken by an anomaly, and the remaining symmetries are spontaneously broken in the following ways. For fermions in a complex representation:

$$SU(n_f) \otimes SU(n_f) \rightarrow SU(n_f); \quad (\text{III.19})$$

for fermions in a real representation:

$$SU(2n_f) \rightarrow O(2n_f); \quad (\text{III.20})$$

and for fermions in a pseudoreal representation:

$$SU(2n_f) \rightarrow Sp(2n_f). \quad (\text{III.21})$$

(See Refs. [22, 38] for more details.) The generators of the broken symmetries become massless Nambu–Goldstone bosons. Since  $SU(n_f)$  has  $n_f^2 - 1$  generators,  $O(n_f)$  has  $n_f(n_f - 1)/2$  generators, and  $Sp(n_f)$  has  $n_f(n_f + 1)/2$  generators, we see that in the three-color, three fundamental-quark case there will be 8 Nambu–Goldstone bosons (a meson octet); in the four-color, two antisymmetric-quark case there will be 9 Nambu–Goldstone bosons (a triplet each of mesons, diquarks, and antidiquarks); and in the two-color, two fundamental-quark case there will be 5 Nambu–Goldstone bosons (a triplet of mesons, a diquark, and an antidiquark).

In addition, recall that if the quarks in these theories are not precisely massless, then the massless Nambu–Goldstone bosons will become instead small-mass, pseudo-Nambu–Goldstone bosons. In our spectra, we are free to vary the mass of these lightest particles to see what effects this will have on the equation of state of the theories. This is especially interesting for lattice practitioners. We discuss this further in Section V.

## IV. MATCHING THE PQCD AND HRG EQUATIONS OF STATE

To match the two asymptotic equations of state, we employ the same technique on the  $T$  axis as on the  $\mu$  axis. As such, let us introduce the symbol  $F$  to stand for either  $T$  or  $\mu$  so that we may discuss the matching in full generality.

To perform the matching, we assume that at the phase-transition point the pressures of the two phases are equal; and we use the thermodynamic constraints that the pressure of a system must increase with  $F$

$$P(F + \Delta F) \geq P(F), \quad (\text{IV.1})$$

and that above a phase-transition point, the physical phase is the one with the higher pressure. We also add a bag constant  $B$  to the pQCD pressure so that

$$P_{\text{pQCD}}(F) = P_{\text{pQCD}}^0(F) + B, \quad (\text{IV.2})$$

where  $P_{\text{pQCD}}^0$  is given by either (II.6)-(II.11) or (II.14). In the plots that follow, we solve the following set of two equations with two unknowns (for a given  $\bar{\Lambda}$ ):

$$P_{\text{HRG}}(F_0) = P_{\text{pQCD}}(F_0, B_0), \quad (\text{IV.3})$$

$$\left. \frac{dP_{\text{HRG}}(F)}{dF} \right|_{F=F_0} = \left. \frac{\partial P_{\text{pQCD}}(F, B_0)}{\partial F} \right|_{F=F_0}. \quad (\text{IV.4})$$

The second of these equations amounts to assuming that the phase transition is of second order. Less restrictive schemes can be implemented as well, such as truncating the HRG and pQCD equations of state far from the transition region and interpolating using the thermodynamic constraint (IV.1) as well as other phenomenological assumptions (see Refs. [39, 40] for examples of this). By varying  $\bar{\Lambda}$  between  $\pi T$  and  $4\pi T$  for the case  $F = T$  and between  $\mu/2$  and  $2\mu$  in the case  $F = \mu$ , (IV.3)-(IV.4) allows us to obtain a region of possible equations of state in the  $(F, P)$  plane for each theory.

## V. RESULTS

In Figure 1, we overlay the bands for the pressure and trace anomaly  $\epsilon - 3P$  (with  $\epsilon$  the energy density) at  $\mu = 0$  that we calculate in the three-color, three-massless-quark case with lattice data from the Budapest–Marseille–Wuppertal Collaboration [2] and the HotQCD Collaboration [3] in their respective regions of validity. We observe that the lattice data agree reasonably well with the band resulting from our HRG+pQCD calculation, both for the pressure as well as for the trace anomaly.

In Figure 2, we show the HRG+pQCD pressure and trace-anomaly bands at  $\mu = 0$  for all four theories with the  $T$  axis scaled by the critical temperature  $T_c$ , which we define to be the average of the matching temperatures for the upper and lower edge of our pQCD band to the HRG equation of state.  $T_c$  should thus be regarded as an estimate of the confinement-deconfinement critical temperature. We list the explicit values obtained in HRG+pQCD in Table I. We see that once the temperature axis has been scaled by  $T_c$ , all the theories show similar behavior both for the pressure and trace anomaly, a phenomenon that is well-known from pure-gauge theories [41]. The differences at low temperatures are due to the different numbers of Nambu–Goldstone bosons with zero quark mass in the two-color and four-color theories (see Section III B or Appendix A) and the fact that in the real world there are only pseudo-Nambu–Goldstone bosons. We tested this by increasing the mass of the lightest (now pseudo-) Nambu–Goldstone bosons, which qualitatively changed the shape of the pressure curves until they matched that of the real-world, three-color theory.

In Figure 3, we show the pressure and trace-anomaly bands at  $T = 0$  for all four theories with the  $\mu$  axis scaled by the critical chemical potential  $\mu_c$ , again, defined to be the average of the matching chemical potential of the upper and lower edge of our pQCD band to the HRG equation of state. The value of  $\mu_c$  should be regarded as an estimate for the confinement-deconfinement transition, whereas the critical chemical potential for the onset transition would be given by the smallest value of  $m_i/r_i$ , to use the notation of Section III. In the fundamental theories, this value of  $m_i/r_i$  corresponds to the lightest baryon mass. Similar to the  $\mu = 0$  case, the  $\mu \neq 0, T = 0$  results show similar trends when scaled appropriately. Again, the different behaviors at low  $\mu/\mu_c$  are due to the fact that there are Nambu–Goldstone bosons composed solely of quarks in the two-color fundamental and four-color antisymmetric theories. Again, this was tested by increasing the masses of the lightest particles.

The values of  $T_c/\sqrt{\sigma}$  and  $\mu_c/\sqrt{\sigma}$  for our HRG+pQCD calculations are given in Table I. While the results suggests that the  $T_c$  values for the different theories are within 20 percent of each other, the extracted  $\mu_c$  values span a much broader range.

We stress that in the four-color antisymmetric case with  $\Lambda_{\overline{\text{MS}}}/\sqrt{\sigma} = 0.723$ , we were unable to carry out our matching procedure at  $\mu = 0$  in the chiral limit. We found that in this case, the HRG pressure rose too sharply and never intersected the pQCD pressure-band. Thus, we have only plotted the  $\Lambda_{\overline{\text{MS}}}/\sqrt{\sigma} = 0.527$  results for the four-color antisymmetric theory in our figures. We feel this is justified for a few reasons. First of all, the values of  $\mu_c$  are equal within uncertainties for the two different values of  $\Lambda_{\overline{\text{MS}}}/\sqrt{\sigma}$ . Secondly, in the case where  $\Lambda_{\overline{\text{MS}}}/\sqrt{\sigma} = 0.723$ , we were able to carry out our HRG+pQCD matching procedure when we increased the mass of the lightest bosons (the pion mass). By varying the pion mass, we were able to extrapolate to the chiral limit, obtaining a value of  $\mu_c/\sqrt{\sigma} = 0.3$ , which agrees with the value found for  $\Lambda_{\overline{\text{MS}}}/\sqrt{\sigma} = 0.527$ . In light of this agreement, and in light of how the four-color antisymmetric theory was the only theory where our matching was strained, we conjecture that the true value of  $\Lambda_{\overline{\text{MS}}}/\sqrt{\sigma}$  in this case is closer to the pure-gluon value than it is in the real-world, three-color case. We point out that this prediction could be tested in future lattice-gauge-theory calculations.

Finally, we have calculated the speed of sound  $c_s$  at  $T = 0$  in all four QCD-like theories using our HRG+pQCD scheme, shown in Figure 5. We note that in some cases,  $c_s$  exceeds the speed of light, and thus these particular matching results from HRG+pQCD should be considered unphysical (a standard constraint when using cold-nuclear-matter equations of state). Nevertheless, our results indicate that it is generally possible to obtain physical equations of state wherein  $c_s^2 > 1/3$  for all fundamental QCD-like theories. This finding could be of interest because restricting  $c_s^2 < 1/3$  has previously been noted to be in tension with astrophysical observations [42]. Again, we point out that this is a property which could be tested in future lattice-gauge-theory calculations.

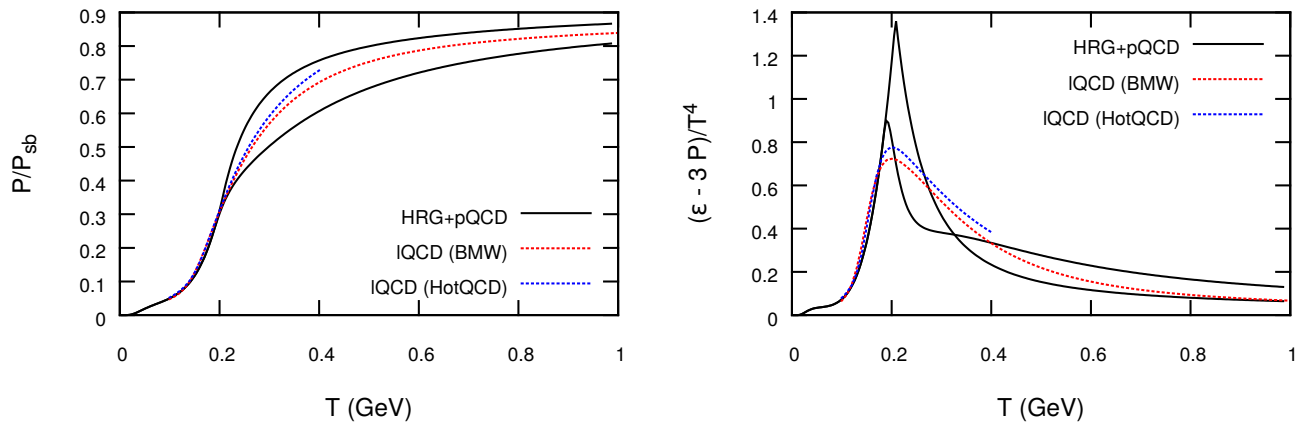


FIG. 1: Normalized pressure (left) and trace anomaly (right) at  $\mu = 0$  for the three-color, three-massless-quark case from HRG+pQCD in comparison to lattice-QCD data from the Budapest–Marseille–Wuppertal Collaboration [2] and the HotQCD Collaboration [3].

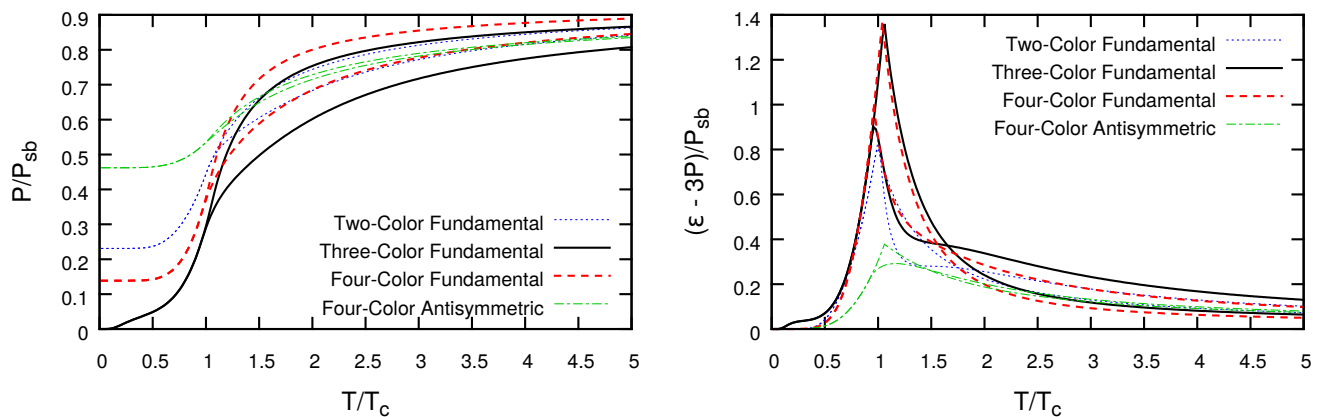


FIG. 2: Normalized pressure (left) and trace anomaly (right) at  $\mu = 0$  for the two-color, three-color, four-color fundamental, and four-color antisymmetric theories in HRG+pQCD. Note that the  $T$  axis has been scaled by the critical temperature (see main text).

<i>Group, Representation, <math>n_f</math></i>	$T_c/\sqrt{\sigma}$	$\mu_c/\sqrt{\sigma}$
SU(2), fundamental, 2	0.400	3.24
SU(3), fundamental, 3	0.47	2.382
SU(4), fundamental, 2	0.44	2.853
SU(4), antisymmetric, 2 ( $\Lambda_{\overline{MS}}/\sqrt{\sigma} = 0.527$ )	0.29	5.09
SU(4), antisymmetric, 2 ( $\Lambda_{\overline{MS}}/\sqrt{\sigma} = 0.723$ )	no matching	5.0

TABLE I: The ratios  $T_c/\sqrt{\sigma}$  and  $\mu_c/\sqrt{\sigma}$  for the theories analyzed in this paper. Errors are given by the number of significant figures.

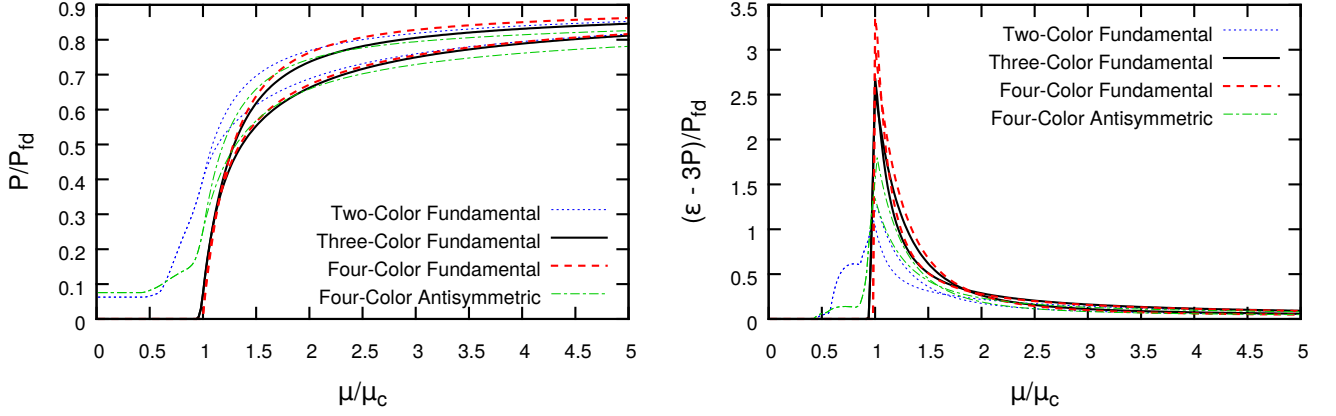


FIG. 3: Normalized pressure (left) and trace anomaly (right) at  $T = 0$  for the two-color, three-color, four-color fundamental, and the four-color antisymmetric theories in HRG+pQCD. Note that the  $\mu$  axis has been scaled by the critical chemical potential (see main text).

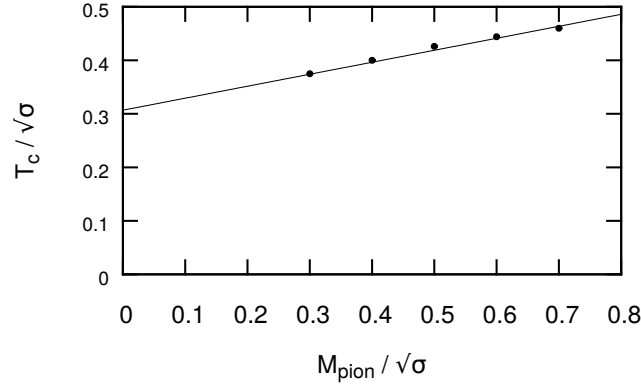


FIG. 4: Deconfinement-transition temperature  $T_c$  as a function of pion mass for the four-color, antisymmetric theory in the  $\mu = 0$ ,  $\Lambda_{\overline{\text{MS}}}/\sqrt{\sigma} = 0.723$  case. The straight line is a fit to the results where matching could be performed, and defines the extrapolation to the chiral limit (see main text).

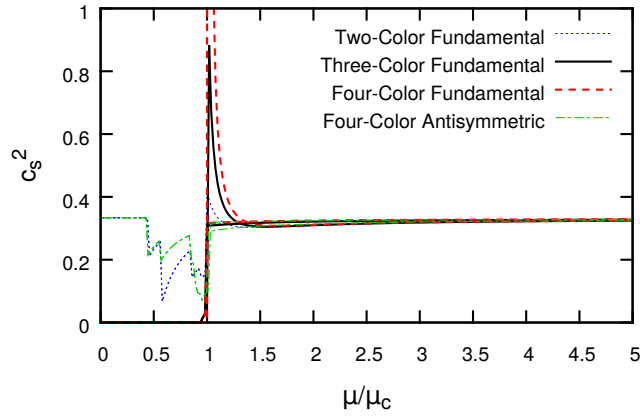


FIG. 5: The speed of sound squared at  $T = 0$  for the two-color, three-color, four-color fundamental, and the four-color antisymmetric theories in HRG+pQCD. Note that the  $\mu$  axis has been scaled by the critical chemical potential (see main text).

## VI. CONCLUSIONS

We have calculated the equation of state at non-zero temperatures and densities in a first-principles approach: by matching physics from the hadron resonance gas at low energies to perturbative QCD at high energies for two-, three-, and four-color ‘QCD’. In particular, our work provides predictions for results in future lattice studies at zero temperature and non-zero chemical potential for two-color QCD with two fundamental fermions and four-color QCD with two flavors of fermions in the two-index, antisymmetric representation. While some aspects of our study are systematically improvable, we expect the current HRG+pQCD results to be sufficiently robust that a direct comparison with future lattice-QCD studies in the two- and four-color cases could validate or rule out the HRG+pQCD method, depending on the quantitative agreement. In the case of agreement, one could thus also reasonably expect HRG+pQCD results to be quantitatively accurate in the physically-relevant, three-color-QCD case.

To make our results accessible, we have made them electronically available [43].

## ACKNOWLEDGMENTS

We thank Gert Aarts, Tom DeGrand, Simon Hands, Yuzhi Liu, Marco Panero, Andreas Schmitt, and Aleksii Vuorinen for helpful discussions and suggestions. This work was funded by the Department of Energy, DoE award No. [de-sc0008132](#).

### Appendix A: Particle Tables

Mesons			(continued)			Baryons		
Mass/ $\sqrt{\sigma}$	Spin	Isospin	Mass/ $\sqrt{\sigma}$	Spin	Isospin	Mass/ $\sqrt{\sigma}$	Spin	Isospin
0.00	0	1	3.65	1	1	0.00	0	0
1.43	0	0	3.92	2	0	1.43	0	0
1.60	1	1	3.93	1	0	1.86	1	1
1.86	1	0	3.98	2	1	2.79	1	1
2.79	1	0	3.98	3	0	3.26	0	0
3.02	2	0	4.02	3	1	3.06	1	0
3.06	1	0	4.05	1	1	3.02	2	0
3.08	0	0	4.25	0	1	3.92	2	0
3.10	1	1	4.25	0	0	3.93	1	1
3.14	2	1	4.35	1	1	3.98	3	1
3.25	1	1	4.35	1	0	4.88	4	0
3.26	0	0	4.86	4	1	3.08	0	0
3.38	1	0	4.88	4	0	3.38	1	1
3.50	0	1	5.00	1	1	5.00	1	1
3.50	0	1	5.00	1	0	4.25	0	0
						4.35	1	0

TABLE II: The included particle spectrum in the two-color fundamental theory.

## Mesons

Mass/ $\sqrt{\sigma}$	Spin	Isospin
0.00	0	1
1.43	0	0
1.83	1	1
1.86	1	0
2.33	0	1
2.79	1	0
2.94	1	1
3.00	1	1
3.02	2	0
3.06	1	0
3.08	0	0
3.10	0	1
3.14	2	1
3.26	0	0
3.38	1	0
3.45	1	1
3.45	0	1
3.90	1	1
3.92	2	0
3.93	1	0
3.98	2	1
3.98	3	0
4.02	3	1
4.05	1	1
4.25	0	0
4.35	1	0
4.86	4	1
4.88	4	0
5.00	1	1
5.00	1	0

## Baryons

Mass/ $\sqrt{\sigma}$	Spin	Isospin
2.84	0	1
3.05	1	3
3.47	2	5
2.84	0	5
3.05	1	5
3.47	2	5
3.05	1	3
3.47	2	3
4.10	3	3

TABLE III: The included particle spectrum in the four-color fundamental theory.

## Mesons

Mass/ $\sqrt{\sigma}$	Spin	Isospin
0.00	0	1
1.43	0	0
1.83	1	1
1.86	1	0
2.33	0	1
2.79	1	0
2.94	1	1
3.00	1	1
3.02	2	0
3.06	1	0
3.08	0	0
3.10	0	1
3.14	2	1
3.26	0	0
3.38	1	0
3.45	1	1
3.45	0	1
3.90	1	1
3.92	2	0
3.93	1	0
3.98	2	1
3.98	3	0
4.02	3	1
4.05	1	1
4.25	0	0
4.35	1	0
4.86	4	1
4.88	4	0
5.00	1	1
5.00	1	0

## Diquarks

Mass/ $\sqrt{\sigma}$	Spin	Isospin
0.00	0	1
1.43	0	1
1.86	1	0
2.79	1	0
3.02	2	1
3.06	1	1
3.08	0	1
3.26	0	1
3.38	1	0
3.92	2	1
3.93	1	0
3.98	3	0
4.25	0	1
4.35	1	1
4.88	4	1
5.00	1	0

## Baryons

Mass/ $\sqrt{\sigma}$	Spin	Isospin
0.71	0	0
1.55	1	1
3.24	2	2
5.77	3	3

TABLE IV: The mesons, diquarks, and baryons in the four-color antisymmetric theory. (See Table V for remaining particles in this theory.)

Tetraquarks, di-mesons,  
and diquark-mesons

(continued)

Mass/ $\sqrt{\sigma}$	$g_{\text{Spin}}$	$g_{\text{Isospin}}$
0.00	1	1
1.43	1	1
1.86	3	3
2.79	3	3
2.86	1	1
3.02	5	5
3.06	3	3
3.08	1	1
3.26	1	1
3.29	3	3
3.38	3	3
3.72	9	9
3.92	5	5
3.93	3	3
3.98	7	7
4.21	3	3
4.25	1	1
4.35	3	3
4.45	5	5
4.49	3	3
4.51	1	1
4.65	9	9
4.69	1	1
4.81	3	3
4.88	9	9
4.89	15	15
4.92	9	9
4.95	3	3
5.00	3	3
5.12	3	3
5.24	9	9
5.35	5	5
5.36	3	3
5.40	7	7

Mass/ $\sqrt{\sigma}$	$g_{\text{Spin}}$	$g_{\text{Isospin}}$
5.57	9	9
5.68	1	1
5.78	18	18
5.79	9	9
5.81	15	15
5.84	21	21
5.85	9	9
5.87	3	3
6.05	28	28
6.08	15	15
6.11	5	5
6.11	3	3
6.12	9	9
6.14	3	3
6.17	10	10
6.21	9	9
6.29	5	5
6.31	9	9
6.32	3	3
6.35	1	1
6.40	15	15
6.43	3	3
6.44	9	9
6.46	3	3
6.52	1	1
6.64	3	3
6.70	15	15
6.71	9	9
6.74	27	27
6.76	30	30
6.86	9	9
6.94	25	25
6.95	15	15
6.98	15	15

(continued)

Mass/ $\sqrt{\sigma}$	$g_{\text{Spin}}$	$g_{\text{Isospin}}$
6.99	9	9
7.00	40	40
7.01	3	3
7.04	24	24
7.06	7	7
7.14	9	9
7.18	5	5
7.19	3	3
7.24	7	7
7.27	5	5
7.30	15	15
7.31	12	12
7.33	1	1
7.36	21	21
7.37	15	15
7.41	9	9
7.43	3	3
7.51	1	1
7.61	3	3
7.63	3	3
7.67	27	27
7.73	9	9
7.79	9	9
7.83	25	25
7.85	15	15
7.86	9	9
7.89	35	35
7.90	66	66
7.94	27	27
7.95	49	49
7.96	9	9
8.02	15	15
8.06	9	9
8.08	3	3

(continued)

Mass/ $\sqrt{\sigma}$	$g_{\text{Spin}}$	$g_{\text{Isospin}}$
8.14	9	9
8.17	5	5
8.18	3	3
8.23	7	7
8.26	30	30
8.27	15	15
8.28	9	9
8.33	21	21
8.38	9	9
8.50	1	1
8.60	3	3
8.70	9	9
8.80	45	45
8.81	27	27
8.86	63	63
8.92	15	15
8.93	9	9
8.98	21	21
9.13	9	9
9.23	27	27
9.25	3	3
9.35	9	9
9.76	81	81
9.88	27	27

TABLE V: The included tetraquarks, di-mesons, and diquark-mesons in the four-color antisymmetric theory. (There is one of each of these particle types for each line in this table.) Here,  $g_{\text{Spin}}$  and  $g_{\text{Isospin}}$  are the total spin and isospin degeneracies, respectively. As noted above in Section III, we need not determine how all of the four-quark-object degrees of freedom break up into spin and isospin multiplets because of the mass degeneracy.

- 
- [1] Borsanyi, Szabolcs and Endrodi, Gergely and Fodor, Zoltan and Jakovac, Antal and Katz, Sandor D. and others. The QCD equation of state with dynamical quarks. *JHEP*, 1011:077, 2010.
- [2] Szabolcs Borsanyi, Zoltan Fodor, Christian Hoelbling, Sandor D. Katz, Stefan Krieg, et al. Full result for the QCD equation of state with 2+1 flavors. *Phys.Lett.*, B730:99–104, 2014.
- [3] A. Bazavov and others (HotQCD Collaboration). Equation of state in (2+1)-flavor QCD. *Phys.Rev.*, D90(9):094503, 2014.
- [4] Marco Cristoforetti, Francesco Di Renzo, and Luigi Scorzato. New approach to the sign problem in quantum field theories: High density QCD on a Lefschetz thimble. *Phys.Rev.*, D86:074506, 2012.
- [5] Gert Aarts, Lorenzo Bongiovanni, Erhard Seiler, Denes Sexty, and Ion-Olimpiu Stamatescu. Controlling complex Langevin dynamics at finite density. *Eur.Phys.J.*, A49:89, 2013.
- [6] Dnes Sexty. Simulating full QCD at nonzero density using the complex Langevin equation. *Phys.Lett.*, B729:108–111, 2014.
- [7] Gert Aarts, Erhard Seiler, Denes Sexty, and Ion-Olimpiu Stamatescu. Simulating QCD at nonzero baryon density to all orders in the hopping parameter expansion. 2014.
- [8] Gert Aarts, Felipe Attanasio, Benjamin Jger, Erhard Seiler, Denes Sexty, et al. QCD at nonzero chemical potential: recent progress on the lattice. 2014.
- [9] Philippe de Forcrand, Jens Langelage, Owe Philipsen, and Wolfgang Unger. The lattice QCD phase diagram in and away from the strong coupling limit. *Phys.Rev.Lett.*, 113:152002, 2014.
- [10] Mikko Laine and York Schroder. Quark mass thresholds in QCD thermodynamics. *Phys.Rev.*, D73:085009, 2006.
- [11] Pasi Huovinen and Pter Petreczky. QCD Equation of State and Hadron Resonance Gas. *Nucl.Phys.*, A837:26–53, 2010.
- [12] Aleks Kurkela, Paul Romatschke, and Aleks Vuorinen. Cold Quark Matter. *Phys.Rev.*, D81:105021, 2010.
- [13] Jens Langelage, Gernot Munster, and Owe Philipsen. Strong coupling expansion for finite temperature Yang-Mills theory in the confined phase. *JHEP*, 0807:036, 2008.
- [14] A. Vuorinen. The Pressure of QCD at finite temperatures and chemical potentials. *Phys.Rev.*, D68:054017, 2003.
- [15] K. Kajantie, M. Laine, K. Rummukainen, and Y. Schroder. The Pressure of hot QCD up to  $g_6 \ln(1/g)$ . *Phys.Rev.*, D67:105008, 2003.
- [16] K. Kajantie, M. Laine, K. Rummukainen, and Y. Schroder. Four loop vacuum energy density of the  $SU(N(c)) +$  adjoint Higgs theory. *JHEP*, 0304:036, 2003.
- [17] J.P. Blaizot, E. Iancu, and A. Rebhan. On the apparent convergence of perturbative QCD at high temperature. *Phys.Rev.*, D68:025011, 2003.
- [18] Najmul Haque, Aritra Bandyopadhyay, Jens O. Andersen, Munshi G. Mustafa, Michael Strickland, et al. Three-loop HTLpt thermodynamics at finite temperature and chemical potential. *JHEP*, 1405:027, 2014.
- [19] Eric Braaten and Agustin Nieto. Free energy of QCD at high temperature. *Phys.Rev.*, D53:3421–3437, 1996.
- [20] T. van Ritbergen, J.A.M. Vermaseren, and S.A. Larin. The Four loop beta function in quantum chromodynamics. *Phys.Lett.*, B400:379–384, 1997.
- [21] Simon Hands, Seyong Kim, and Jon-Ivar Skullerud. Deconfinement in dense 2-color QCD. *Eur.Phys.J.*, C48:193, 2006.
- [22] J.B. Kogut, Misha A. Stephanov, D. Toublan, J.J.M. Verbaarschot, and A. Zhitnitsky. QCD - like theories at finite baryon density. *Nucl.Phys.*, B582:477–513, 2000.
- [23] J.I. Kapusta and Charles Gale. *Finite-temperature field theory: Principles and applications*. 2006.
- [24] K.A. Olive et al. Review of Particle Physics. *Chin.Phys.*, C38:090001, 2014.
- [25] Harvey B. Meyer and Michael J. Teper. Glueball Regge trajectories and the pomeron: A Lattice study. *Phys.Lett.*, B605:344–354, 2005.
- [26] Biagio Lucini and Gregory Moraitis. The Running of the coupling in  $SU(N)$  pure gauge theories. *Phys.Lett.*, B668:226–232, 2008.
- [27] Patrick Fritzscht, Francesco Knechtli, Bjorn Leder, Marina Marinkovic, Stefan Schaefer, et al. The strange quark mass and Lambda parameter of two flavor QCD. *Nucl.Phys.*, B865:397–429, 2012.
- [28] Gunnar S. Bali, Francis Bursa, Luca Castagnini, Sara Collins, Luigi Del Debbio, et al. Mesons in large-N QCD. *JHEP*, 1306:071, 2013.
- [29] Simon Hands, Peter Sitch, and Jon-Ivar Skullerud. Hadron Spectrum in a Two-Colour Baryon-Rich Medium. *Phys.Lett.*, B662:405–412, 2008.
- [30] Randy Lewis, Claudio Pica, and Francesco Sannino. Light Asymmetric Dark Matter on the Lattice:  $SU(2)$  Technicolor with Two Fundamental Flavors. *Phys.Rev.*, D85:014504, 2012.
- [31] Gregory S. Adkins, Chiara R. Nappi, and Edward Witten. Static Properties of Nucleons in the Skyrme Model. *Nucl.Phys.*, B228:552, 1983.
- [32] Elizabeth Ellen Jenkins. Baryon hyperfine mass splittings in large N QCD. *Phys.Lett.*, B315:441–446, 1993.
- [33] Thomas DeGrand. Lattice baryons in the  $1/N$  expansion. *Phys.Rev.*, D86:034508, 2012.
- [34] T. Appelquist et al. Composite bosonic baryon dark matter on the lattice:  $SU(4)$  baryon spectrum and the effective Higgs interaction. *Phys.Rev.*, D89:094508, 2014.
- [35] Thomas DeGrand, Yuzhi Liu, Ethan Neil, Yigal Shamir, and Benjamin Svetitsky. Spectroscopy of  $SU(4)$  gauge theory with two flavors of sextet fermions. To appear.
- [36] Thomas DeGrand, Yuzhi Liu, Ethan T. Neil, Yigal Shamir, and Benjamin Svetitsky. Spectroscopy of  $SU(4)$  lattice gauge theory with fermions in the two index anti-symmetric representation. 2014.

- [37] Stefano Bolognesi. Baryons and Skyrmions in QCD with Quarks in Higher Representations. *Phys.Rev.*, D75:065030, 2007.
- [38] Michael E. Peskin. The Alignment of the Vacuum in Theories of Technicolor. *Nucl.Phys.*, B175:197–233, 1980.
- [39] Kurkela, Aleksi and Fraga, Eduardo S. and Schaffner-Bielich, Jürgen and Vuorinen, Aleksi. Constraining neutron star matter with Quantum Chromodynamics. *Astrophys.J.*, 789:127, 2014.
- [40] Toru Kojo, Philip D. Powell, Yifan Song, and Gordon Baym. Phenomenological QCD equation of state for massive neutron stars. 2014.
- [41] Marco Panero. Thermodynamics of the QCD plasma and the large-N limit. *Phys.Rev.Lett.*, 103:232001, 2009.
- [42] Paulo F. Bedaque and Andrew W. Steiner. Sound velocity bound and neutron stars. 2014.
- [43] The results may be obtained from the web page of one of the authors, <http://hep.itp.tuwien.ac.at/~paulrom/>.